Jordan Journal of Civil Engineering, Volume **1**, No. **1**, **2007**

pH-Dependence and Contributions of The Carbonic Species To Co_2 Flux Across The Gas/Liquid Interface

Abdallah Shanableh
Chairman-Department of Civil Engineering, Coordinator-Hazards and Engineering Risk Management Research Group
University of Sharjah, P.O.Box 27272, Sharjah, United Arab Emirates, shanableh@sharjah.ac.ae

ABSTRACT

The purpose of this article is to expand the available knowledge on CO_2 transfer across the gas/liquid interface in two ways: (1) propose a new mathematical model to describe the pH dependence of CO_2 flux across the gas/liquid interface; and (2) propose new relationships that quantitatively describe the contributions of each of the carbonate species (H_2CO_3, HCO_3^-, and CO_3^{2-}) to total flux across the gas/liquid interface. The new model was based on accounting for the difference between the pH in the liquid phase at any time during gas transfer and the pH of the liquid phase at equilibrium when net gas transfer stops. The article also proposes a correction to the currently in-use mathematical model, which was found to apply in the special change and in unlikely cases in which the initial pH does not change. The theoretical and experimental work presented in this article present clear theoretical and mathematical understanding of the process of gas transfer involving acid-base ionization reactions. Numerous batch and continuous-flow countercurrent reactors CO_2 stripping experiments were conducted at different initial pH values to verify the proposed model. The experiments included runs in which the pH was allowed to change as a result of CO_2 transfer and experiments involving buffered solutions in which the pH did not change significantly. In all cases, the experimental results matched the theory in an excellent manner.

KEYWORDS: *Carbon dioxide transfer across the gas/liquid interface, CO_2 stripping, CO_2 absorption, pH-dependant gas transfer, mathematical CO_2 transfer rate model, contributions of carbonate species CO_2 transfer.*

1.0 INTRODUCTION

Carbon dioxide is a key ingredient of the global carbon cycle and is constantly undergoing physical, chemical, and biochemical transformations in the environment. Carbon dioxide exchange across the gas/liquid interface is an important process in the carbon cycle and is of great multidisciplinary interest in the scientific community. The relationship between CO_2 transfer and the pH of the liquid phase is an extremely important concept which has numerous and wide-ranging implications in natural and man-made systems (Seibel and Walsh, 2003, Guinotte et al., 2006, Luttge, 2002, kuihara, 2004, Sabine et al., 2004).

The rate of CO_2 exchange is highly pH dependent, with CO_2 stripping requiring low pH levels and CO_2 absorption requiring high pH levels. The driving force for the exchange is the lack of CO_2 equilibrium between the

Received on 1/12/2006 and Accepted for Publication on 18/12/2006.

gas and liquid phases on both sides of the interface. The state of equilibrium is described by Henry's law, as in Equation 1.

$$CO_{2G.Eq} = HCO_{2L.Eq} \quad (1)$$

where $CO_{2G.Eq}$ = concentration of CO_2 in the gaseous bulk phase, $CO_{2L.Eq}$ = equilibrium or saturation concentration of CO_2 in the liquid phase, and H=Henry's law constant.

Henry's constant is dimensionless in Equation 1 when CO_{2G} and $CO_{2L.Eq}$ are expressed in identical units (i.e., mass/volume). While the CO_2 transfer rate-pH relationship is of vital importance, a general mathematical model to describe that the relationship does not exist. Instead, researchers (Onda et al, 1972, Perry and Green, 1984, Talbot et al., 2000, House et al., 1984) resort to determining the value of the mass transfer co-efficient (K_La) in the general gas transfer reaction rate (Equation 2) at a given pH using empirical, pH-independent, models or using curve-fitting of experimental data or correlating K_La values for CO2 and other gases, as oxygen.

$$r_T = \pm K_L^* a(C_{TL} - C_{TL.Eq}) \quad (2)$$

where r_T =CO_2 transfer reaction rate, C_{TL} = total carbonates concentration in the liquid phase, $K_L^* a$ is the overall mass transfer coefficient, $C_{TL.Eq}$ = equilibrium concentration of total carbonates in the liquid phase, and $(C_{TL} - C_{TL.Eq})$ is the gas transfer driving force.

The only available mathematical model to describe the relationship between CO_2 transfer rate and pH was presented by Howe and Lawler (1989. It was based on the two-film gas transfer theory (Lewis and Whitman, 1924) and theoretical proposals by Stumm and Morgan (1981). The model accounts for the pH dependency of the CO_2 transfer rate across the gas/liquid interface in a simple manner through changes proposed to the driving force. The model is presented in Equation 3, below.

$$r_T = \pm \alpha_{oL} K_L a(C_{TL} - C_{TL.Eq}) \quad (3)$$

where α_{oL} =H_2CO_3 fraction of the total carbonates concentration (C_{TL}) in the liquid phase (α_{oL} is a function of the pH only) and $\alpha_{oL} K_L a = K_L^* a$.

Unfortunately, the analysis presented in this article demonstrates that the model described in Equation 2 applies only in a special case. Using sufficiently buffered solutions so that the initial pH did not significantly change as a result of CO_2 transfer, the model described in Equation 2 provided excellent representation of the pH-dependence of CO_2 removal in laboratory batch and continuous-flow experiments (Howe and Lawler, 1989). Nevertheless, the model is invalid as a general model to describe CO_2 transfer and applies only in the special and unlikely case in which the initial pH does not change.

This article presents a general model to describe the pH-dependence of CO_2 transfer across the gas/liquid interface. Furthermore, new mathematical relationships are proposed to describe the contribution of each of the carbonate species (H_2CO_3, HCO_3^-, and CO_3^{2-}) to total flux across the gas/liquid interface. The mathematical model was verified using numerous laboratory experiments which validated the theory. The model can easily be integrated into gas transfer design and analysis procedures. Equations for application of the model to CO_2 transfer systems are also given. The article also present useful experimental data related to the relationship between the pH and CO_2 transfer across the gas/liquid interface.

2.0 MODEL DEVELOPMENT

2.1 Acid-Base Ionization of the Carbonate System

The theory of speciation of the carbonate system is well established. The following review is meant to clarify the terminology used in this article. The carbonate

species, H_2CO_3, HCO_3^-, and CO_3^{2-}, are involved in instantaneous equilibrium reactions among each other. The equilibrium molar concentration of the total carbonates species in solution is equal to $C_{TL} = [H_2CO_3] + [HCO_3] + [CO_3]$. The relative abundance of each of the carbonate species is pH dependant, where $[H_2CO_3] = \alpha_{oL} C_{TL}$, $[HCO_3] = \alpha_{1L} C_{TL}$, and $[CO_3] = \alpha_{2L} C_{TL}$ HCO_3^-. The fractions α_{oL}, α_{1L}, and α_{2L} depend only on the pH and can be calculated from Equations 4 to 6.

$$\alpha_{oL} = \left(1 + \frac{k_1}{[H]} + \frac{k_1 k_2}{[H]^2}\right) \quad (4)$$

$$\alpha_{1L} = \left(1 + \frac{[H]}{k_1} + \frac{k_2}{[H]}\right) \quad (5)$$

$$\alpha_{2L} = \left(1 + \frac{[H]}{k_2} + \frac{[H]^2}{k_1 k_2}\right) \quad (6)$$

where k_1 is the equilibrium constant for the ionization reaction: $H_2CO_3 = HCO_3^- + H^+$, and k_2 is the equilibrium constant for the ionization reaction: $HCO_3^- = CO_3^{2-} + H^+$.

2.2 CO2 Exchange Steps and the Two-Film Theory

Carbon dioxide transfer across the gas/liquid interface can be described by a dynamic equilibrium reaction in which the two opposite gas transfer processes, CO_2 absorption and stripping, occur continuously and simultaneously. When the rate of stripping is greater than the rate of absorption, a net removal of CO_2 from the liquid is achieved, and visa versa. Dynamic equilibrium occurs when the rate of stripping is equal to the rate of absorption. When CO_2 from the gas phase is absorbed into solution, it forms aqueous CO_2 (CO_2^*), which becomes hydrated forming H_2CO_3, as depicted in Figure 1. H_2CO_3 is part of the carbonate system and is involved in rapid and dynamic acid-base dissociation/association ionization reactions with the other carbonate species, HCO_3^- and CO_3^{2-}. When CO_2 is released from aqueous solutions into the gaseous phase, the process is reversed, as depicted in Figure 1.

Carbon dioxide absorption and stripping involve a number of steps. Within the liquid phase, three processes that may lead to CO_2 exchange across the gas/liquid interface during stripping or absorption. The three processes are:

1. Hydration or de-hydration of aqueous CO_2 (CO_2^* + $H_2O = H_2CO_3$);
2. Acid-base dissociation/association reactions; and
3. Transportation (i.e., diffusion) of carbonate species towards or away from the gas/liquid interface.

The overall rate of CO_2 exchange across the gas/liquid interface is controlled by the slowest of these three steps. We come to realize that of the three processes, the rate of attainment of ionization equilibrium (dissociation/ association of the carbonate species) is instantaneous, while in comparison the rates of attainment of hydration (dehydration) and diffusion are slow (Stumm and Morgan, 1981; Howe and Lawler, 1989). The differences in the rates of diffusion, hydration (or dehydration) and ionization are important consideration in developing the rate of CO_2 exchange and establishing the contributions of each of the carbonate components to CO_2 transfer across the gas/liquid interface.

According to the well accepted two-film theory (Lewis and Whitman, 1924), two layers, a liquid film and a gas film, are assumed to form on both sides of the gas/liquid interface during gas transfer. The flux of molecules that occurs across the liquid and gas films is driven by the respective concentration gradient (ΔC) across each layer or film. The total flux, F_T, across each film is determined by Fick's first law (Equation 7). The negative sign is because flux occurs from high to low concentrations.

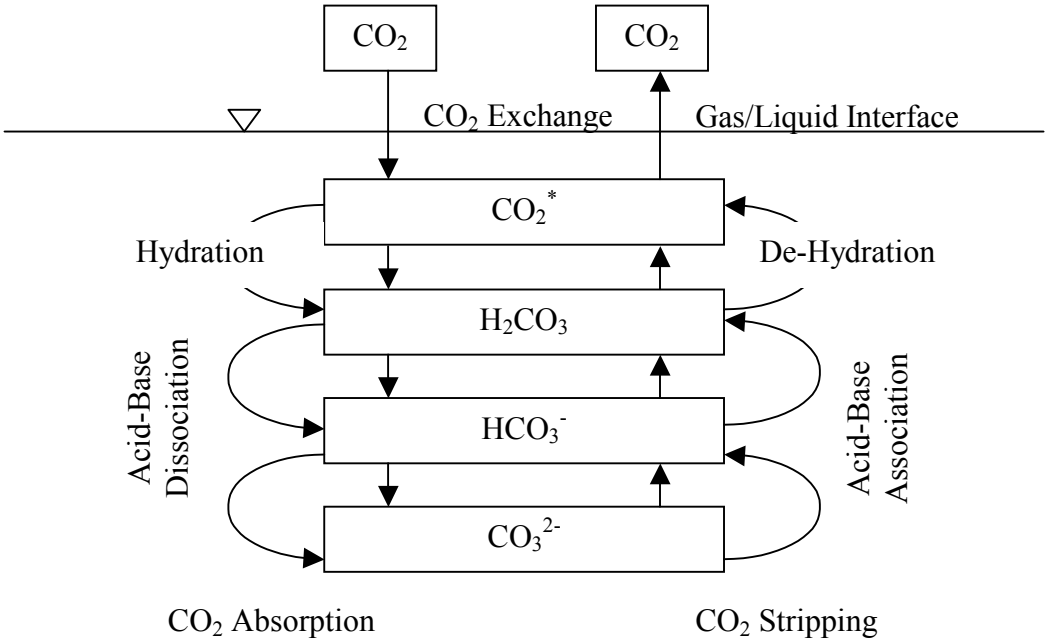

Fig. 1. Depiction of CO_2 transfers across the gas/liquid interface.

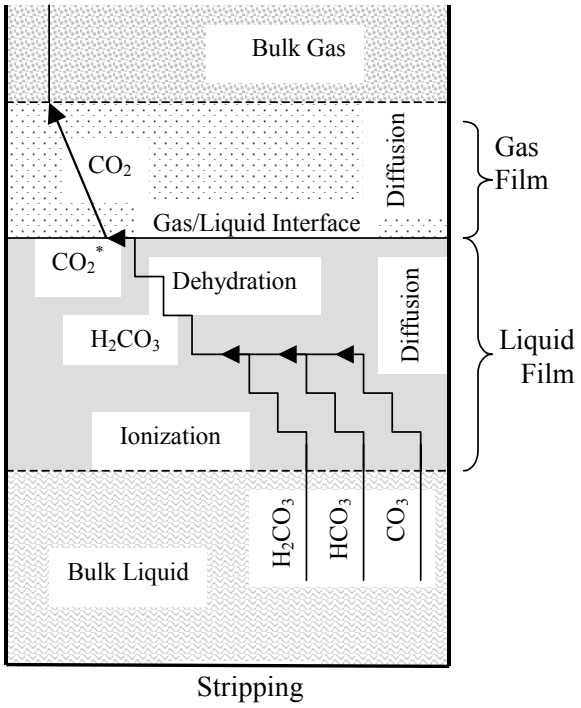

Fig. 2. Conceptual representation of CO_2 stripping through the two films surrounding the gas/liquid interface. Three processes occur in the liquid film: (1) diffusion of molecules towards the interface; (2) acid-base reactions converting CO_3 and HCO_3 into H_2CO_3; and (3) dehydration of H_2CO_3 into aqueous CO_2^*.

$$F_T = -K_m \Delta C \quad (7)$$

where F_T = total flux with units of mass/(area-time), K_m = mass transfer coefficient for a specific medium (i.e., water, air) with units of length/time, and ΔC = concentration gradient with units of mass/length^3.

During gas transfer, a concentration gradient for CO_2 exists in the liquid phase between the gas/liquid interface and the bulk liquid. Concentration gradients also exist for each of the carbonate species which are being transported towards or away from the gas/liquid interface. As the carbonate species move towards and away from the interface, instantaneous ionization reactions take place to maintain equilibrium in response to the addition or removal of CO_2. The process is depicted in Figure 2 for stripping, which shows stepwise ionization and dehydration reactions in the liquid film.

During stripping, flux as defined by Fick's law (Equation 7), occurs in the liquid and gas films driven by the corresponding concentration gradients for CO_2 across the liquid and gas films, as expressed in Equations 8 and 9.

$$F_{LStripping} = K_l (CO_{2L} - CO_{2L.Int}) \quad (8)$$

$$F_{GStripping} = K_g (CO_{2G.Int} - CO_{2G.Eq}) \quad (9)$$

where, F_L = flux across the liquid film, F_G = flux across the gas film, $CO_{2L.Int}$ = concentration of aqueous CO_2 in the liquid at the gas/liquid interface, CO_{2L} = concentration of CO_2 (i.e., H_2CO_3) in the bulk liquid, $CO_{2G.Int}$ = concentration of CO_2 in the gas phase at the interface, and $CO_{2G.Eq}$ = concentration of CO_2 in the bulk gas phase (as defined by Henry's law in Equation 1), and K_L and K_g = liquid and gas phase transfer coefficients.

At steady-state, flux across the liquid film is equal to flux across the gas film (i.e., $F_{LStripping}=F_{GStripping}=F_{Stripping}$). The equality of flux on both sides of the gas/liquid interface is described in Equation 10.

$$K_l (CO_{2L} - CO_{2L.Int}) = K_g (CO_{2G.Int} - CO_{2G.Eq}) \quad (10)$$

The two-film theory is based on assuming that the concentration of the gas in the liquid at the interface is in equilibrium (i.e., saturation) with the concentration of the gas in the gaseous phase. The equilibrium relationship is described by Henry's relationship (Equation 11).

$$CO_{2G.Int} = HCO_{2L.Int} \quad (11)$$

Substituting for $CO_{2G.Int}$ and $CO_{2G.Eq}$ from Equations 1 and 11 into Equation 10, then solving for $CO_{2L.Int}$ results in Equation 12. Then substituting for $CO_{2L.Int}$ from Equations 12 into Equation 8 results in Equation 13.

$$CO_{2L.Int} = \frac{K_l CO_{2L} + HK_g CO_{2L.Eq}}{K_l + HK_g} \quad (12)$$

$$F_{Stripping} = \frac{HK_g K_l}{K_l + HK_g} (CO_{2L} - CO_{2L.Eq}) \quad (13)$$

By letting $K_L = HK_g K_l / (K_l + HK_g)$ and noting that $CO_{2L} = \alpha_{oL} C_{TL}$ and $CO_{2L.Eq} = \alpha_{oL.Eq} C_{TL.Eq}$, the general flux equation during stripping can be expressed as in Equation 14. A similar Equation 15 applies for CO_2 absorption.

$$F_{Stripping} = K_L (\alpha_{oL} C_{TL} - \alpha_{oL.Eq} C_{TL.Eq}) \quad (14)$$

$$F_{Absorption} = K_L (\alpha_{oL.Eq} C_{TL.Eq} - \alpha_{oL} C_{TL}) \quad (15)$$

The gas transfer rate can be obtained by multiplying the flux in Equations 14 and 15 by the specific surface area (a) of contact between the gas and liquid phases at the interface. The result is the general gas transfer rate equation (Equation 16).

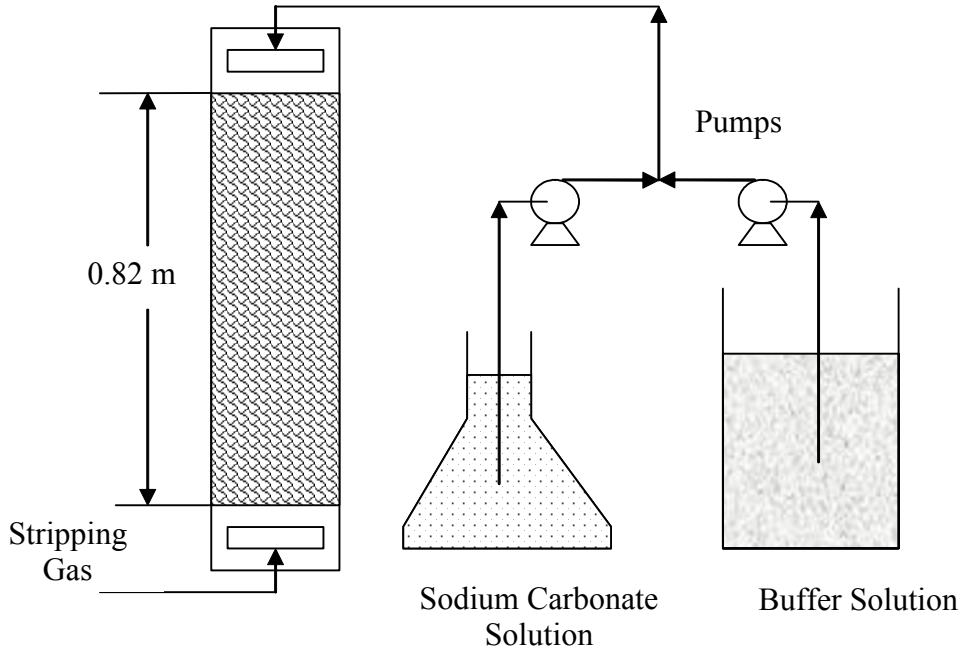

Fig. 3. Simplified schematic of the continuous-flow counter-current CO_2 stripping column

$$r_T = \pm K_L a(\alpha_{oL} C_{TL} - \alpha_{oL.Eq} C_{TL.Eq}) \quad (16)$$

It is important at this point to note the difference between α_{oL} and $\alpha_{oL.Eq}$. α_{oL} is a function of the actual pH of the bulk liquid at any time during gas transfer, while $\alpha_{oL.Eq}$ is a future value and is a function of the pH of the liquid at the time equilibrium is achieved. In fact, α_{oL} and $\alpha_{oL.Eq}$ can not be considered equal unless the pH remains unchanged or equilibrium, as described by Henry's law, is achieved.

2.3 Simplification of CO_2 Transfer Rate Equation under Special Conditions

While the removal or addition of CO_2 to solution affects the pH. As the pH can be assumed to remain unchanged in well-buffered solutions or when the pH changes are small. At constant pH, the gas transfer rate in Equation 16 can be rewritten as in question 17. Equation 17 is the same as the model proposed by Howe and Lawler (1989), which clearly applies to the special case in which the pH remains constant.

$$r_T = \pm \alpha_{oL} K_L a(C_{TL} - C_{TL.Eq}) \quad (17)$$

Using a clean gas to remove CO_2 from the liquid phase at steady pH further simplifies the gas transfer rate. Assuming that the concentration of CO_2 in the stripping gas does not change significantly, the term representing the equilibrium concentration $(C_{TL.Eq})$ can be neglected and the gas transfer rate becomes as follows:

$$r_T = \pm \alpha_{oL} K_L a C_{TL} \quad (18)$$

The above theory was tested using batch and continuous flow CO_2 stripping experiments. Obviously, the special case presented in Equation 2 is capable of representing previously published data (i.e., Howe and Lawler, 1989) in exactly the same manner.

2.4 Contributions of the Carbonate Species to Total Flux

The flux of CO_2 across the gas/liquid interface is matched with an equivalent flux of the carbonate species to compensate for the loss or gain of aqueous $^*CO_2$. The total flux is equal to the flux of the three carbonate species, as in Equation 19. Note that $(\alpha_{oL} + \alpha_{1L} + \alpha_{2L}) = 1$. The same equation was also proposed by Stumm and organ (1981) who stopped short of quantifying the pH dependency of CO_2 transfer across the gas/liquid interface.

$$F_T = F_{H_2CO_3} + F_{HCO_3} + F_{CO_3} = \alpha_{oL}F_T + \alpha_{1L}F_T + \alpha_{2L}F_T = F_T(\alpha_{oL} + \alpha_{1L} + \alpha_{2L}) \quad (19)$$

where, $F_{H_2CO_3}$ *= flux due to* H_2CO_3, F_{HCO_3} *= flux due to* HCO_3^-, *and* F_{CO_3} *= flux due to* CO_3^{2-}.

Accordingly, the contribution of each of the carbonate species to total flux can be described according to Equations 20-22.

$$F_{H_2CO_3} = \pm\alpha_o K_L(\alpha_{oL}C_{TL} - \alpha_{oL.Eq}C_{TL.Eq}) \quad (20)$$

$$F_{HCO_3} = \pm\alpha_1 K_L(\alpha_{oL}C_{TL} - \alpha_{oL.Eq}C_{TL.Eq}) \quad (21)$$

$$F_{CO_3} = \pm\alpha_2 K_L(\alpha_{oL}C_{TL} - \alpha_{oL.Eq}C_{TL.Eq}) \quad (22)$$

3.0 EXPERIMENTAL EVALUATION

Simple and numerous laboratory-scale batch and continuous-flow stripping experiments were conducted to generate data reproducing the well-known pH-dependency of CO_2 stripping. The batch experiments were conducted in a 15 cm Diameter x 40 cm height cylinder filled with five liters carbonate solution. Two solutions were prepared: one containing 0.05 M phosphate buffer and the other without buffer. The stripping experiments were conducted at different initial pH values. The initial pH was adjusted to the desired level using HCl and NaOH solutions. The initial total inorganic carbon in each solution was approximately 100 mg/L. Helium was used for stripping at a steady flow rate. During each experiment, the total inorganic carbon concentration (C_{TL}) and the pH were measured with time.

The counter-current, continuous-flow, packed column stripping experiments were conducted in a 15 cm Diameter x 100 cm height cylinder (Figure 3) filled with plastic media to a depth of 82 cm. Two sets of experiments were conducted, one using a buffered carbonate solution (0.05 M phosphate buffer) and the other without phosphate buffer. The liquid stream was introduced at the top of the column at a controlled rate. Air was introduced at the bottom of the column, and the flow of air was maintained at a controlled rate. The experiments were conducted at different initial pH values, and the pH and inorganic carbon concentration in samples collected from the column influent and effluent were measured over a period of time and the steady-state results were used in the analysis. For some experiments, additional side-stream samples were taken at 0.18 m, 0.39 m and 0.6 m along the column.

4.0 RESULTS AND DISCUSSION

The purpose of the experimental evaluation was to verify the theory developed in the model development section. In particular, the purpose was to test the general mathematical model, $r_T = \pm K_L a(\alpha_{oL}C_{TL} - \alpha_{oL.Eq}C_{TL.Eq})$, proposed to account for the pH-dependency of the gas transfer rate. Starting with the simplest case, which involved stripping CO_2 from the buffered solution in batch-reactor experiments, two simplifying assumptions (as in Equation 18) were used to analyze the data. These are: (1) that the pH did not change significantly; and (2) that CO_2 concentration in the stripping gas (Argon) did not change significantly. To analyze the experimental results obtained using the batch reactor, Equation 18,

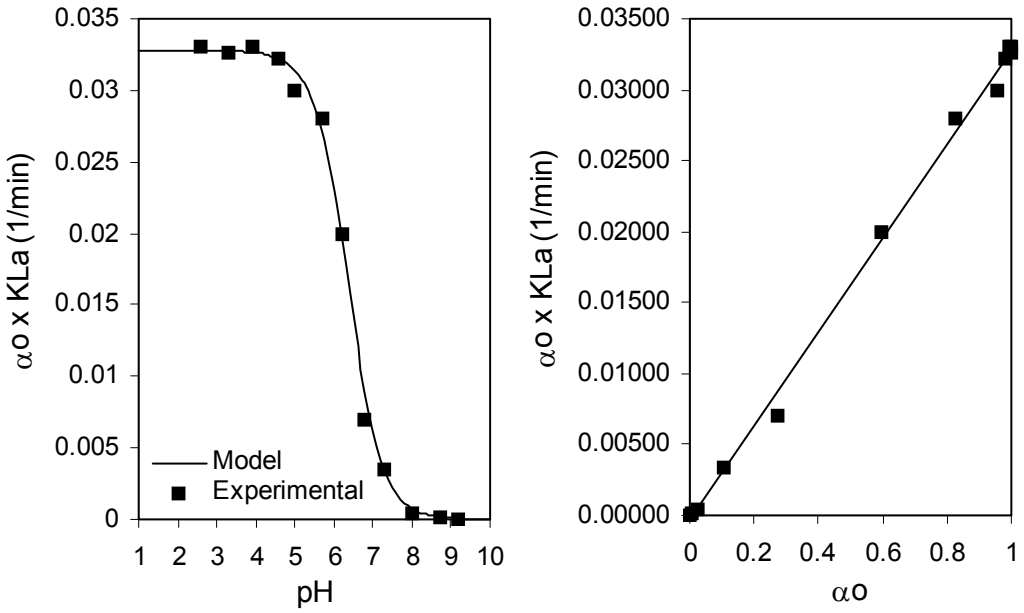

Fig. 4. Dependence of the reaction rate constant ($\alpha_{oL}K_La = K_L^*a$) on the pH in the buffered batch stripping experiments. The figure on the right shows K_La as independent of pH.

which represents a special case of the general model, was applied. Noting that $r_T = dC_{TL}/dt$, where t = reaction time, and integrating Equation 18 results in Equation 23.

$$\ln C_{TL} = \ln C_{TL_{Initial}} - \alpha_{oL}K_La.t \quad (23)$$

Based on Equation 23, $\alpha_{oL}K_La$ was determined as the slope of the line of best-fit expressing the linear relationship between $\ln C_{TL}$ versus time (t). The result indicated that as expected, the mathematical model provided excellent representation of the experimental data, as shown in Figure 3. It should be noted that $\alpha_{oL}K_La$ includes two terms, K_La, one is independent of pH and α_{oL}, the other is a function of pH only (Figure 3).

Results similar to those obtained using the batch reactor were also achieved in the counter-current reactor stripping experiments, which involved using the phosphate buffer to minimize pH change due to CO_2 stripping. Based on the special case described in Equation 17 at constant pH, the differential equation that describes the removal of CO_2 from any section of the column with dh height (i.e., $dh = Q_L dt/A$, where A = column area, Length^2 and Q_L=liquid flow rate, length^3/time) can be re-written as.

$$\frac{\alpha_{oL}AK_La}{Q_L}dh = \frac{dC_{TL}}{(C_{TL} - C_{TL.Eq})} \quad (24)$$

Noting that $CO_{2G.Eq} = \alpha_{oL}HC_{TL.Eq}$, a mass balance on the bottom section of the column can be used to estimate a value for $C_{TL.Eq}$ for substitution in Equation 24, which yields:

$$Q_G(CO_{2GInitial} - CO_{2G.Eq}) = Q_L(C_{TL.Effluent} - C_{TL}) \quad (25)$$

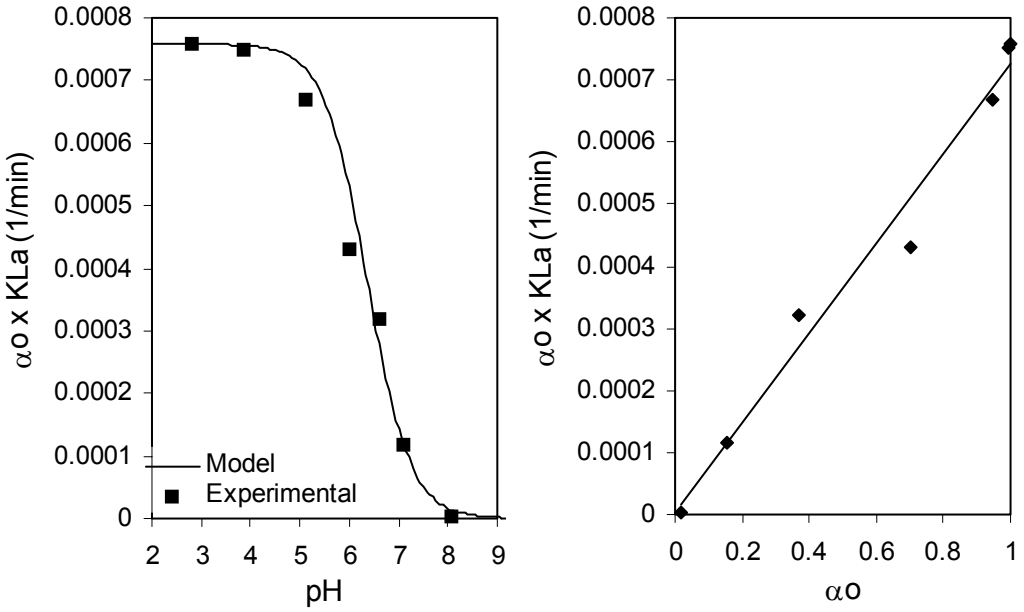

Fig.5. Dependence of the reaction rate constant ($\alpha_{oL}K_La = K_L^*a$) on the pH in the buffered continuous-flow stripping experiments. The figure shows K_La as independent of pH.

$$\frac{\alpha_{oL}AK_La}{Q_L}dh = \frac{dC_{TL}}{\left(\frac{R-1}{R}\right)C_{TL} - \frac{CO_{2GInitial}}{\alpha_{oL}H} + \frac{1}{R}C_{TL.Effluent}} \tag{26}$$

where Q_G =gas flow rate (length^3/time), $CO_{2GInitial}$ = initial concentration of CO_2 in the gas phase, $C_{TL.Effluent}$ = total carbonates concentration in the final effluent, and $R = \alpha_{oL}HQ_G/Q_L$ is the stripping factor.

At steady-state, integration of Equation 26 yields the counter-current stripping Equation 27.

$$\alpha_{oL}K_La = \frac{Q_LR}{Ah(R-1)}Ln\left[\frac{1}{R} + \frac{(R-1)}{R}\left(\frac{C_{TL.Initial} - \frac{CO_{2GInitial}}{\alpha_{oL}H}}{C_{TL.Effluent} - \frac{CO_{2GInitial}}{\alpha_{oL}H}}\right)\right] \tag{27}$$

The data in Figure 4 is a direct application of Equation 27 at different initial pH values. The value of $\alpha_{oL}K_La$ for each experimental run was determined from Equation 27. Similar to the batch reactor treatment, the results provided good representation of the expected pH-dependence of the CO_2 stripping rate. Once again, $\alpha_{oL}K_La$ includes two terms, K_La, which is independent of pH and α_{oL}, which is a function of pH only (Figure 4).

The theoretical pH change can be estimated from Equation 28, which approximates the initial alkalinity of solutions buffered with phosphates and carbonates. Equation 28 can be re-written as Equation 29, in terms of the relevant pH dependant fractions α_{1L} and α_{2L} for the carbonate system and α_{1LP}, α_{2LP} and α_{3LP} for the phosphates system. It is well known that the initial alkalinity does not change as a result of CO_2 transfer, however the pH does change. Also in Equations 28 and 29, the total phosphates concentration (C_{TP}) does not change but only the total carbonates (C_{TL}) concentration changes as a result of CO_2 stripping. The initial alkalinity

can be estimated from the initial pH, initial total carbonates concentration and initial total phosphates concentration. The final pH can then be estimated from the remaining concentration of total carbonates and from the unchanged total phosphates concentration.

$$Alk_{Initial} = [OH^-] + [HCO_3^-] + 2[CO_3^{2-}] + [H_2PO_4^-] + [HPO_4^{2-}] + [PO_4^{3-}] - [H] \quad (28)$$

$$Alk_{Initial} = \frac{k_w}{[H]} + (\alpha_{1L} + 2\alpha_{2L})C_{TL} + (\alpha_{1LP} + 2\alpha_{2LP} + 3\alpha_{3LP})C_{TP} - [H] \quad (29)$$

In the experiments conducted using the phosphate buffer, the measured and estimated theoretical pH values indicate that the pH did actually change as a result of CO_2 stripping in the phosphate buffered solutions by as much as 0.4 pH units, depending on the initial pH. While the pH change may not be highly significant in buffered solutions, the general gas transfer rate model in Equation 16 should not be based on equating the pH of the bulk liquid at any time during gas transfer with the pH to be achieved at equilibrium.

Next, the results of the remaining two sets of experiments in which no phosphate buffer was used to control pH change during stripping are discussed. In these experiments, the pH was allowed to increase as a result of CO_2 stripping. At this stage, it is important to re-emphasize the difference between α_{oL} and $\alpha_{oL.Eq}$ in the general gas transfer model in Equation 16. α_{oL} is a function of the actual pH of the bulk liquid at any time during gas transfer, while $\alpha_{oL.Eq}$ is a future value and is a function of the pH of the liquid at the time equilibrium is achieved. In fact, α_{oL} and $\alpha_{oL.Eq}$ can not be considered equal unless the pH remains unchanged or equilibrium, as described by Henry's law, is achieved.

In the variable pH batch stripping experiments in which Argon was used as the stripping gas, Equation 18 applies. However, because both α_{oL} and C_{TL} are variable, direct integration of the reaction rate equation is not possible. Instead, numerical integration can easily be used, as follows:

$$\frac{\Delta C_{TL}}{\Delta t} = -\alpha_{oL} K_L a C_{TL} \quad (30)$$

As discussed previously, while the removal of CO_2 increases the pH, the initial alkalinity does not change. The alkalinity, expressed in terms of molar concentrations of the relevant ingredients, is presented in Equation 31. Solving Equation 29 for C_{TL} then substituting the value of C_{TL} into Equation 28 results in a relationship between the change in C_{TL} and the pH, as expressed in Equation 32.

$$Alk_{Initial} = \frac{k_w}{[H]} + (\alpha_{1L} + 2\alpha_{2L})C_{TL} - [H] \quad (31)$$

$$\frac{\Delta C_{TL}}{\Delta t} = -\alpha_{oL} K_L a \left(\frac{[H] Alk_{Initial} - k_w + [H]^2}{[H](\alpha_{1L} + 2\alpha_{2L})} \right) \quad (32)$$

Equations 30 and 32 were used to determine the K_La values using the measured pH and C_{TL} values with time. Initially, a value for K_La was estimated for one of the experimental runs as follows: the first $\Delta C_{TL(1)}$ was estimated using the initial alkalinity ($Alk_{Initial}$), initial pH ($pH_{Initial}$), initial carbonate concentration ($C_{TLInitial}$), a chosen small value for Δt, and assuming a value for K_La. The second $\Delta C_{TL(2)}$ was estimated using the same K_La, $C_{TL(1)} = C_{TL.Initial} - \Delta C_{TL(1)}$, $Alk_{Initial}$, and a new value for pH calculated from the alkalinity Equation 31 at $C_{TL(1)}$. The process was repeated until $\sum \Delta t = t_{total}$, with the final concentration $(C_{TL(final)} = C_{TL.(final-1)} - \Delta C_{TL(final)})$ compared with the measured $C_{TL.Effluent}$. The iterative process was repeated using new values for K_La until the measured and estimated effluent concentrations became

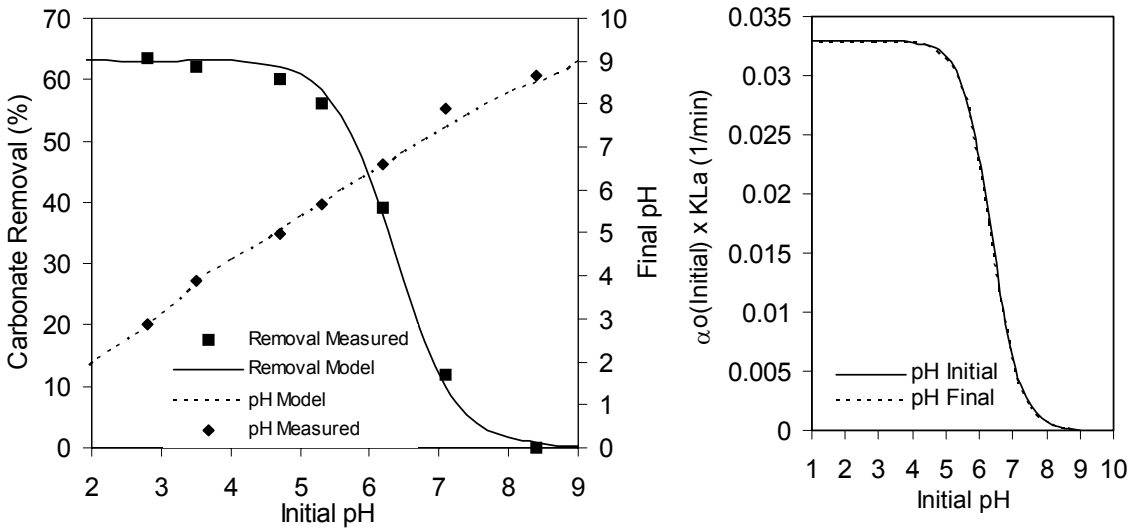

Fig. 6. (Left) Carbonate removal and pH change as a result of batch CO_2 stripping for 30 minutes without the use of phosphate buffer. (Right) Dependence of the reaction rate constant ($\alpha_{oL} K_L a = K_L^* a$) on the initial pH

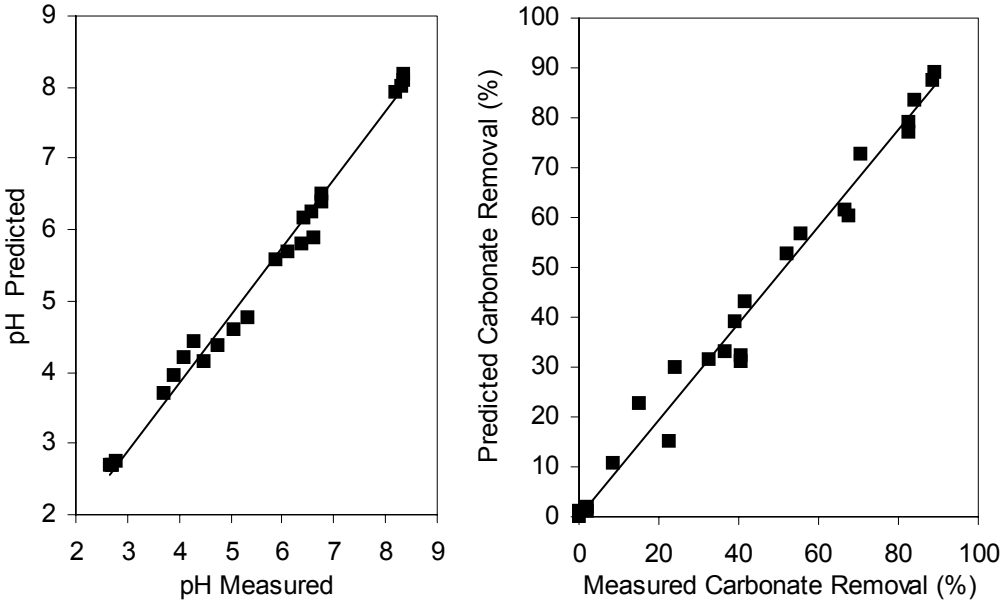

Fig. 7. Predicted versus measured performance of CO_2 stripping from the non-buffered solutions in the stripping counter-current column.

equal. For the other experimental runs conducted at the different initial pH values, the known K_La value, which is pH independent, was used estimate the effluent pH and C_{TL} using Equations 30-32, which were then compared with the measured values as presented in Figure 5.

The experimental results and model predictions in Figure 5 matched each other in an excellent manner. As expected, CO_2 stripping resulted in carbonate removals that were highly dependant on the pH. In addition, comparison of the influent and effluent pH values reveals that the pH change due to CO_2 stripping varied in the range of less than 0.1 to as high as 0.9 units, depending on the degree of CO_2 removal and initial pH. The results in Figure 5 also show $\alpha_{oLInitial}K_La$, that includes two terms, K_La, one is independent of pH and α_{oL}, other is a function of pH. However, the initial pH was used in this case to represent $\alpha_{oLInitial}K_La$.

The final set of experiments involved the use of the continuous-flow counter-current stripping column to remove CO_2 without the use of phosphate buffer. In this case, the column Equation 26 and alkalinity Equation 31 apply as follows:

$$\frac{\alpha_{oL}AK_La}{Q_L}\Delta h=\frac{\Delta C_{TL}}{\left(\frac{R-1}{R}\right)C_{TL}-\frac{CO_{2GInitial}}{\alpha_{oL}H}+\frac{1}{R}C_{TL.Effluent}} \tag{33}$$

$$C_{TL}=\frac{[H]^2+Alk_{Initial}[H]-k_w}{[H](\alpha_{1L}+2\alpha_{2L})} \tag{34}$$

Because the pH is allowed to change, numerical integration simultaneously by using Equations 33 and 34 permits estimation of the pH and C_{TL} along the column. In this case, the solution target was the achievement of an effluent C_{TL} equal to the measured effluent C_{TL}. Starting with the influent concentration and pH, using small Δh increments, and assuming a value for K_La, ΔC_{TL} can be estimated and new values for C_{TL} and pH are estimated. The procedure is continued and the estimated effluent concentration is compared with the measured effluent concentration, with the calculations repeated using a new value for K_La if both concentrations were not equal. Additional pH and C_{TL} measurements were taken along the column at various depths, and those were compared with the model predictions, as in Figure 6. The data in Figure 6 proves one more time that the model provided excellent representation of the measured data, which further confirms the validity of the proposed general gas transfer rate model.

Equations 19-22 describe the contribution of each of the carbonate species to total flux across the gas/liquid interface. The contributions of the carbonate species to total flux is equal to α_{oL} for H_2CO_3 ($F_{H_2CO_3}/F_T=\alpha_{oL}$), α_{1L} for HCO_3^- ($F_{H_2CO_3}/F_T=\alpha_{1L}$) and α_{2L} for CO_3^{2-} ($F_{CO_3}/F_T=\alpha_{2L}$). The fraction of total flux contributed by each of the carbonate species as a function of pH reflects the abundance of that particular species, as shown in Figure 7 (left). Within the specific pH range of $pH<pk_1$ (i.e., $k_1=10^{-6.3}$ $pk_1=6.3$), H_2CO_3 is the most abundant and as such makes the dominant contribution to the flux of the carbonate species. In the range $pk_1<pH<pk_2$, (i.e., $k_2=10^{-10.3}$ $pk_2=10.3$) HCO_3^- is the most abundant and dominates flux, and CO_3^{2-} is the most abundant and dominates flux when $pH>pk_2$. It should be noted that while HCO_3^- and CO_3^{2-} dominate flux at pH values greater that pk_1, the total flux becomes less than half its maximum value when $pH>pk_1$ and almost negligible when $pH>pk_2$.

When the pH remains significantly unchanged and α_{oL} is considered equal to $\alpha_{oL.Eq}$, a new flux term (F_C), representing the overall carbonate species flux, is introduced for the purposes of this discussion (Equation 35). The way to view F_C is to think of the carbonate

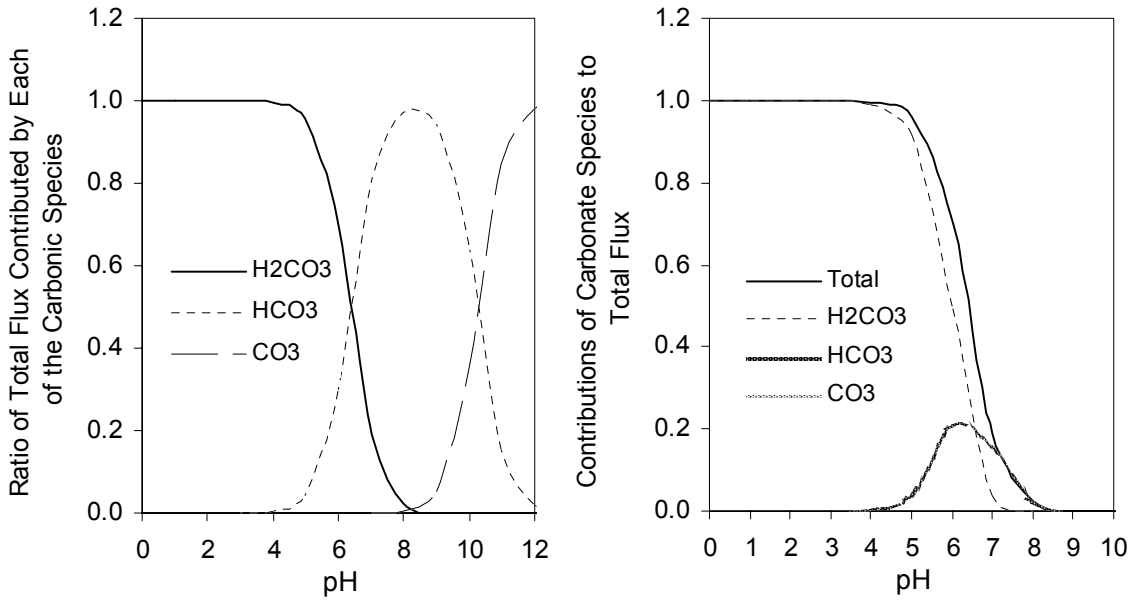

Fig. 8. Ratio and absolute contributions of the various carbonate species to total CO2 transfer rate across the gas/liquid interface.

species as if they were made of one component that does not undergo acid-base ionization reactions, then the flux will be equal to F_C, as follows:

$$F_C = K_L(C_{TL} - C_{TL.Eq}) \tag{35}$$

The relationship between the carbonate species flux and the overall carbonate flux thus can be expressed as in Equations 36-39. The relationships expressed in Equations 36-39 are graphically shown in Figure 7.

$$\frac{F_T}{F_C} = \alpha_{oL} \tag{36}$$

$$\frac{F_{H_2CO_3}}{F_C} = \alpha_{oL}\alpha_{oL} \tag{37}$$

$$\frac{F_{HCO_3}}{F_C} = \alpha_{1L}\alpha_{oL} \tag{38}$$

$$\frac{F_{CO_3}}{F_C} = \alpha_{2L}\alpha_{oL} \tag{39}$$

According to the data presented in Figure 7 (Right), the F_C flux component contributed by H_2CO_3 is the largest and the most important. The F_C component contributed by HCO_3^- starts increasing from a negligible value at a pH of approximately $pk_1 - 2$. At $pH = pk_1$, the F_C components contributed by H_2CO_3 and HCO_3^- become equal, each accounting for approximately 50 percent of the total flux. At pH= pk_1, F_C is at approximately 25% of its maximum observed value. At pH values in the range pk_1 to pk_2, the F_C component contributed by HCO_3^- has the largest value. At pH values greater than pk_2, F_C becomes negligible and dominated by F_{CO_3} contribution. Clearly, the contributions of ionic carbonate species, especially HCO_3^-, enhance F_C. Without enhancement, F_C would have been lower than the typically observed values, especially when the pH is greater than $pk_1 - 2$.

5.0 CONCLUSIONS

A new mathematical model to describe the pH dependence of CO_2 transfer rate (r_T) across the gas/liquid interface was introduced and verified using numerous laboratory experiments. The model was based on quantitatively accounting for the difference between the pH in the liquid phase at any time during gas transfer and the ultimate pH of the liquid phase to be achieved at equilibrium when the net gas transfer stops. The batch and continuous-flow countercurrent reactors CO_2 stripping experiments confirmed the validity of the mathematical CO_2 transfer rate model. The contributions of the various carbonate species to the CO_2 transfer rate across the gas/liquid interface can be described according to their fractions of the total carbonates, or $r_{H_2CO_3} = \alpha_{oBulk} r_{Total}$, $r_{HCO_3} = \alpha_{1Bulk} r_{Total}$, $r_{H_2CO_3} = \alpha_{2Bulk} r_{Total}$.

REFERENCES

Guinotte, J.M., Orr, J., Cairns, S., Freiwald, A., Morgan, L., and George, R. (2006). "Will human-induced changes in seawater chemistry alter the distribution of deep-sea scleractinian corals?." *Front. Ecol. Environ*., 4: 141–146.

House, W., Howard, J. and Skirrow, G. (1984). Kinetics of carbon dioxide transfer across the air/water interface, Faraday Discuss. *Chem. Soc*., 77: 33 – 46.

Howe, K. J., and Lawler, D. F. (1989). "Acid-Base Reactions in Gas Transfer: A Mathematical Approach.". *Journal AWWA*, 81: 61-66.

Kurihara, H., Shimode, S. and Shirayama, Y. (2004). "Sub-lethal effects of elevated concentration of CO_2 on planktonic copepods and sea urchins." *Journal of Oceanography,* 60: 743–750.

Lewis, W. K., and Whitman, W. G. (1924). "Principles of Gas Adsorption." *Ind. and Eng. Chem.* 16: 1215-1224.

Lüttge, U. (2002). "CO_2-concentrating: consequences in crassulacean acid metabolism." Journal of Experimental Botany, 53 (378): 2131-2142.

Onda, K., Takeuchi, H., and Okumoto, Y. (1968). "Mass transfer coefficients between gas and liquid phases in packed columns." *J. Chem. Eng. Jpn.,* 1: 56–62.

Perry, R.H., and Green, D.W. (1984). *Perry's chemical engineers' handbook*, McGraw-Hill, New York.

Sabine, C., Feely, R., Gruber, N., Key, R., Lee, K., Bullister, J., Wanninkhof, R., Wong, C., Wallace, D., Tilbrook, B., Millero, F., Peng, T., Kozyr, A., Ono, T. and Rios, A. (2004). "The oceanic sink for anthropogenic CO_2." Science, 305: 367–371.

Seibel, B. and Walsh, P. (2003). "Biological impacts of deep-sea carbon dioxide injection inferred from indices of physiological performance." *J. Exp. Biol*., 206: 641-650

Stumm, W. and Morgan, J. J. (1981). *Aquatic Chemistry*. John Wiley and Sons, 2nd Ed., New York

Talbot, P.; Gortares, M.P.; Lencki, R.W.; De la Noue, J. (1991). "Absorption of Carbon Dioxide in Algal Mass Culture Systems a Different Characterization Approach." *Biotechnology and Bioengineering,* 37(9):834-842.